Proceedings of the 1993 IEEE/RSJ International Conference on Intelligent Robots and Systems Yokohama, Japan July 26-30, 1993

Internal Dynamics of a Wheeled Mobile Robot

Xiaoping Yun and Yoshio Yamamoto

General Robotics and Active Sensory Perception (GRASP) Laboratory
University of Pennsylvania
3401 Walnut Street, Room 301C
Philadelphia, PA 19104-6228

Abstract — Since the dynamics of a wheeled mobile robot is nonlinear, the feedback linearization technique is commonly used to linearize the input-output map. The input-output linearized system has a nonlinear internal dynamics. In this paper, the internal dynamics of the mobile robot under the look-ahead control is first characterized. The look-ahead control takes the coordinates of a reference point in front of the mobile robot as the output equation. Using a novel Liapunov function, the stability of the internal dynamics is then analyzed. In particular, it is shown that the internal motion of the mobile robot is asymptotically stable when the reference point is commanded to move forward, whereas the internal motion is unstable when the reference point moves backward. Simulation and experimental results are provided to verify the analysis.

1 Introduction

Feedback control of wheeled mobile robots has recently been studied by a number of researchers [1, 2, 3, 4]. Since the dynamics of a wheeled mobile robot is nonlinear, the technique of feedback linearization is commonly used to facilitate the controller design. A wheeled mobile robot is subject to nonholonomic constraints. A nonholonomic control system also has been extensively studied in a more general framework [5, 6, 7, 8]. Because a nonholonomic dynamic system is not input-state linearizable [9], most feedback control methods proposed for wheeled mobile robots use input-output linearization. Even though the closed-loop input-output map of the mobile robot system using those control methods is linear, the system has a nonlinear internal dynamics which is rarely discussed.

In this paper, we study the internal dynamics of a wheeled mobile robot under the look-ahead control. The look-ahead control takes the coordinates of a reference point in front of the mobile robot as the output equation. By using a nonlinear feedback, the input-output map is linearized. A linear feedback is further applied to stabilize the system. With this controller, the reference point can follow any trajectory. Nevertheless, the internal dynamics of this system is not always stable. By properly choosing a state transformation, we first characterize the internal dynamics as well as the zero dynamics of the mobile robot. The zero dynamics is always stable. We then investigate the stability of the internal dynamics when the reference point is commanded to move forward or backward. Using a novel Liapunov function, we show that the internal dynamics is unstable when the reference point moves backwards. While the unstable behavior of the internal motion has been observed early [10], the analysis of the internal dynamics is presented for the first time.

Both simulation and experiment have been conducted to verify the theoretical analysis. In the experiment, the look-ahead control method is implemented on a TRC LABMATE mobile platform. It is observed that when the reference point is commanded to move backward along a straight line, the mobile robot tends to swivel either left or right and to change the heading angle by 180 degrees, depending on minor misalignment of the heading angle or minor variation of floor conditions. The simulation and experimental results are consistent and they confirm that the internal dynamics is unstable when the reference point moves backwards.

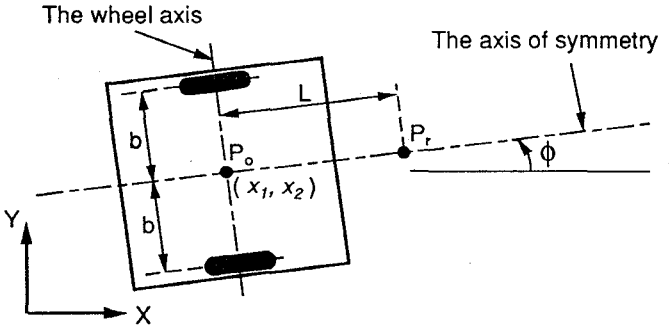

Figure 1: Schematic of the mobile robot.

2 Dynamics of a Wheeled Mobile Robot

2.1 Constraint Equations

In this section, we derive the motion equations and constraint equations of a wheeled mobile robot whose schematic top view is shown in Figure 1. We assume that the mobile robot is driven by two independent wheels and supported by four passive wheels at the corners (not shown in Figure 1). Before proceeding, let us fix some notations (see Figure 1).

- b: the displacement from each of the driving wheels to the axis of symmetry.
- d: the displacement from point P_o to the mass center of the mobile robot, which is assumed to be on the axis of symmetry.
- r: the radius of the driving wheels.
- c: a constant equal to $r/2b$.
- m_c: the mass of the mobile robot without the driving wheels and the rotors of the motors.
- m_w: the mass of each driving wheel plus the rotor of its motor.
- I_c: the moment of inertia of the mobile robot without the driving wheels and the rotors of the motors about a vertical axis through the intersection of the axis of symmetry with the driving wheel axis.
- I_w: the moment of inertia of each driving wheel and the motor rotor about the wheel axis.
- I_m: the moment of inertia of each driving wheel and the motor rotor about a wheel diameter.

0-7803-0823-9/93/$3.00 (C) 1993 IEEE

There are three constraints. The first one is that the mobile robot can not move in lateral direction, *i.e.*,

$$\dot{x}_2 \cos\phi - \dot{x}_1 \sin\phi = 0 \tag{1}$$

where (x_1, x_2) is the coordinates of point P_o in the fixed reference coordinated frame $\mathbf{X}$–$\mathbf{Y}$, and ϕ is the heading angle of the mobile robot measured from $\mathbf{X}$-axis. The other two constraints are that the two driving wheels roll and do not slip:

$$\begin{aligned} \dot{x}_1 \cos\phi + \dot{x}_2 \sin\phi + b\dot{\phi} &= r\dot{\theta}_1 & (2)\\ \dot{x}_1 \cos\phi + \dot{x}_2 \sin\phi - b\dot{\phi} &= r\dot{\theta}_2 & (3) \end{aligned}$$

where θ_1 and θ_2 are the angular positions of the two driving wheels, respectively.

By utilizing the techniques of differential geometry, it turns out that, among the three constraints, two of them are nonholonomic and the third one is holonomic [9].

To obtain the holonomic constraint, we subtract equation (2) from equation (3).

$$2b\dot{\phi} = r(\dot{\theta}_1 - \dot{\theta}_2) \tag{4}$$

Integrating the above equation and properly choosing the initial condition of ϕ, θ_1, and θ_2, we have

$$\phi = c(\theta_1 - \theta_2) \tag{5}$$

which is clearly a holonomic constraint equation. The two nonholonomic constraints are

$$\begin{aligned} \dot{x}_1 \sin\phi - \dot{x}_2 \cos\phi &= 0 & (6)\\ \dot{x}_1 \cos\phi + \dot{x}_2 \sin\phi &= cb(\dot{\theta}_1 + \dot{\theta}_2) & (7) \end{aligned}$$

The second nonholonomic constraint equation in the above is obtained by adding equations (2) and (3). We write these two constraint equations in matrix form

$$A(q)\dot{q} = 0 \tag{8}$$

where

$$q = \begin{bmatrix} q_1 \\ q_2 \\ q_3 \\ q_4 \end{bmatrix} = \begin{bmatrix} x_1 \\ x_2 \\ \theta_1 \\ \theta_2 \end{bmatrix} \tag{9}$$

$$A(q) = \begin{bmatrix} a_{11} & a_{12} & a_{13} & a_{14} \\ a_{21} & a_{22} & a_{23} & a_{24} \end{bmatrix} = \begin{bmatrix} -\sin\phi & \cos\phi & 0 & 0 \\ -\cos\phi & -\sin\phi & cb & cb \end{bmatrix} \tag{10}$$

2.2 Dynamic Equations

We use the Lagrange formulation to establish equations of motion for the mobile robot. The total kinetic energy of the mobile base and the two wheels is

$$K = \frac{1}{2}m(\dot{x}_1^2 + \dot{x}_2^2) + m_c cd(\dot{\theta}_1 - \dot{\theta}_2)(\dot{x}_2 \cos\phi - \dot{x}_1 \sin\phi) + \frac{1}{2}I_w(\dot{\theta}_1^2 + \dot{\theta}_2^2) + \frac{1}{2}Ic^2(\dot{\theta}_1 - \dot{\theta}_2)^2 \tag{11}$$

where

$$\begin{aligned} m &= m_c + 2m_w \\ I &= I_c + 2m_w b^2 + 2I_m \end{aligned}$$

Lagrange equations of motion for the nonholonomic mobile robot system are governed by [11]

$$\frac{d}{dt}\left(\frac{\partial K}{\partial \dot{q}_i}\right) - \frac{\partial K}{\partial q_i} = \tau_i - a_{1i}\lambda_1 - a_{2i}\lambda_2, \qquad i = 1, \ldots 4 \tag{12}$$

where q_i is the generalized coordinate defined in equation (9), τ_i is the generalized force, a_{ij} is from the constraint equation (10), and λ_1 and λ_2 are the Lagrange multipliers. Substituting the total kinetic energy (equation (11)) into equation (12), we obtain

$$\begin{aligned} m\ddot{x}_1 - m_c d(\ddot{\phi}\sin\phi + \dot{\phi}^2\cos\phi) &= \lambda_1 \sin\phi + \lambda_2 \cos\phi & (13)\\ m\ddot{x}_2 + m_c d(\ddot{\phi}\cos\phi - \dot{\phi}^2\sin\phi) &= -\lambda_1 \cos\phi + \lambda_2 \sin\phi & (14)\\ m_c cd(\ddot{x}_2\cos\phi - \ddot{x}_1\sin\phi) + (Ic^2 + I_w)\ddot{\theta}_1 - Ic^2\ddot{\theta}_2 &= \tau_1 - cb\lambda_2 & (15)\\ -m_c cd(\ddot{x}_2\cos\phi - \ddot{x}_1\sin\phi) - Ic^2\ddot{\theta}_1 + (Ic^2 + I_w)\ddot{\theta}_2 &= \tau_2 - cb\lambda_2 & (16) \end{aligned}$$

where τ_1 and τ_2 are the torques acting on the two wheels. These equations can be written in the matrix form

$$M(q)\ddot{q} + V(q,\dot{q}) = E(q)\tau - A^T(q)\lambda \tag{17}$$

where $A(q)$ is defined in equation (10) and

$$M(q) = \begin{bmatrix} m & 0 & -m_c cd\sin\phi & m_c cd\sin\phi \\ 0 & m & m_c cd\cos\phi & -m_c cd\cos\phi \\ -m_c cd\sin\phi & m_c cd\cos\phi & Ic^2 + I_w & -Ic^2 \\ m_c cd\sin\phi & -m_c cd\cos\phi & -Ic^2 & Ic^2 + I_w \end{bmatrix}$$

$$V(q,\dot{q}) = \begin{bmatrix} -m_c d\dot{\phi}^2\cos\phi \\ -m_c d\dot{\phi}^2\sin\phi \\ 0 \\ 0 \end{bmatrix} \qquad E(q) = \begin{bmatrix} 0 & 0 \\ 0 & 0 \\ 1 & 0 \\ 0 & 1 \end{bmatrix}$$

$$\tau = \begin{bmatrix} \tau_1 \\ \tau_2 \end{bmatrix} \qquad \lambda = \begin{bmatrix} \lambda_1 \\ \lambda_2 \end{bmatrix}$$

2.3 State Space Realization

In this subsection, we establish a state space realization of the motion equation (17) and constraint equation (8). Let $S(q)$ be a 4×2 matrix

$$S(q) = [s_1(q) \;\; s_2(q)] = \begin{bmatrix} cb\cos\phi & cb\cos\phi \\ cb\sin\phi & cb\sin\phi \\ 1 & 0 \\ 0 & 1 \end{bmatrix} \tag{18}$$

whose columns are in the null space of $A(q)$ matrix in the constraint equation (8), *i.e.*, $A(q)S(q) = 0$. From the constraint equation (8), the velocity $\dot{q}$ must be in the null space of $A(q)$. It follows that $\dot{q} \in span\{s_1(q), \; s_2(q)\}$, and that there exists a smooth vector $\eta = [\eta_1 \;\; \eta_2]^T$ such that

$$\dot{q} = S(q)\eta \tag{19}$$

and

$$\ddot{q} = S(q)\dot{\eta} + \dot{S}(q)\eta \tag{20}$$

For the specific choice of $S(q)$ matrix in equation (18), we have $\eta = \dot{\theta}$, where $\dot{\theta} = [\dot{\theta}_1 \;\; \dot{\theta}_2]^T$.

Now multiplying the both sides of equation (17) by $S^T(q)$ and noticing that $S^T(q)A^T(q) = 0$ and $S^T(q)E(q) = I_{2\times 2}$ (the 2×2 identity matrix), we obtain

$$S^T(q)M(q)\ddot{q} + S^T(q)V(q,\dot{q}) = S^T(q)E(q)\tau = \tau \tag{21}$$

Substituting equation (20) into the above equation, we have

$$S^T(q)M(q)(S(q)\dot{\eta} + \dot{S}(q)\eta) + S^T(q)V(q,\dot{q}) = \tau \tag{22}$$

By choosing the following state variable

$$x = \begin{bmatrix} x_1 \\ x_2 \\ x_3 \\ x_4 \\ x_5 \\ x_6 \end{bmatrix} = \begin{bmatrix} x_1 \\ x_2 \\ \theta_1 \\ \theta_2 \\ \eta_1 \\ \eta_2 \end{bmatrix} = \begin{bmatrix} q \\ \eta \end{bmatrix} \tag{23}$$

we may represent the motion equation (22) in the state space form

$$\dot{x} = f(x) + g(x)\tau \tag{24}$$

where

$$f(x) = \begin{bmatrix} S\eta \\ -(S^TMS)^{-1}(S^TM\dot{S}\eta + S^TV) \end{bmatrix}, \quad g(x) = \begin{bmatrix} 0 \\ (S^TMS)^{-1} \end{bmatrix}$$

It is noted that the dependent variables for each term have been omitted in the above representation for clarity. All the terms are functions of the state variable x only. Since $\dot{q}$ is not part of the state variable, it is replaced by $S(q)\eta$. To simplify the discussion, we first apply the following state feedback

$$\begin{aligned} \tau &= \alpha^1(x) + \beta^1(x)\mu \\ &= (S^TM\dot{S}\eta + S^TV) + (S^TMS)S^TE\mu \end{aligned} \tag{25}$$

where μ is the new input variable. The closed-loop system becomes

$$\dot{x} = f^1(x) + g^1(x)\mu \tag{26}$$

where

$$f^1(x) = \begin{bmatrix} S\eta \\ 0 \end{bmatrix} \qquad g^1(x) = \begin{bmatrix} 0 \\ I_{2\times 2} \end{bmatrix}$$

3 Look-Ahead Control

It is known that the center point P_o of the mobile robot cannot be controlled by using a static feedback, and that an alternative control method is to control a point in front of the mobile robot [1, 2, 9]. This method is motivated from vehicle maneuvering. When operating a vehicle, a driver looks at a point or an area in front of the vehicle. We define a reference point P_r which is L distance (called look-ahead distance) from P_o (see Figure 1). We take the coordinates of P_r in the fixed coordinate frame as the output equation, *i.e.*,

$$y = h(x) = \begin{bmatrix} x_1 + L\cos\phi \\ x_2 + L\sin\phi \end{bmatrix} \tag{27}$$

To verify if the system is input-output linearizable with this output equation, we compute the derivatives of y.

$$\begin{aligned} \dot{y} &= \frac{\partial h}{\partial x}\dot{x} = \frac{\partial h}{\partial x}\left(f^1(x) + g^1(x)\mu\right) \\ &= \begin{bmatrix} cb\cos\phi - cL\sin\phi & cb\cos\phi + cL\sin\phi \\ cb\sin\phi + cL\cos\phi & cb\sin\phi - cL\cos\phi \end{bmatrix} \begin{bmatrix} \eta_1 \\ \eta_2 \end{bmatrix} = \Phi(x)\eta \end{aligned}$$

Since $\dot{y}$ is not a function of the input μ, we differentiate it once more.

$$\ddot{y} = \Phi(x)\dot{\eta} + \dot{\Phi}(x)\eta = \Phi(x)\mu + \dot{\Phi}(x)\eta$$

The input μ shows up in the second order derivative of y. Clearly, the decoupling matrix in this case is $\Phi(x)$. Since the determinant of $\Phi(x)$ is $(-2c^2bL)$, it is nonsingular as long as the look-ahead distance L is not zero. It follows that the system can be input-output linearized and decoupled [12]. The nonlinear feedback for achieving the input-output linearization and decoupling is

$$\mu = \Phi^{-1}(x)\left(u - \dot{\Phi}(x)\eta\right) \tag{28}$$

Applying this nonlinear feedback, we obtain

$$\ddot{y}_1 = u_1 \tag{29}$$

$$\ddot{y}_2 = u_2 \tag{30}$$

Therefore, the mobile robot can be controlled so that the reference point P_r tracks a desired trajectory. The motion of the mobile robot itself, particularly the motion of the center point P_o, is determined by the internal dynamics of the system which is the topic of the next section.

4 Internal Dynamics

The previous section introduced the look-ahead control method for the mobile robot. In this section, we proceed to study the behavior of the internal dynamics including the zero dynamics of the system. For a general discussion of internal dynamics and zero dynamics, see Chapter 6 of [13] or [14].

We first construct a diffeomorphism by which the overall system can be represented in the norm form of nonlinear systems [13]. Since the relative degree of each output is two, we may construct four components of the needed diffeomorphism from the two outputs and its Lie derivative, *i.e.*, $h_1(x)$, $L_fh_1(x)$, $h_2(x)$ and $L_fh_2(x)$. Since the state variable x is six dimensional, we need two more components. We choose the two components to be θ_1 and θ_2. Thus the proposed diffeomorphic transformation would be

$$z = T(x) = \begin{bmatrix} z_1 \\ z_2 \\ z_3 \\ z_4 \\ z_5 \\ z_6 \end{bmatrix} = \begin{bmatrix} h_1(x) \\ L_fh_1(x) \\ h_2(x) \\ L_fh_2(x) \\ \theta_1 \\ \theta_2 \end{bmatrix} \tag{31}$$

To verify that $T(x)$ is indeed a diffeomorphism, we compute its Jacobian.

$$\frac{\partial T}{\partial x} = \begin{bmatrix} 1 & 0 & -cL\sin\phi & cL\sin\phi & 0 & 0 \\ 0 & 0 & * & * & cb\cos\phi - cL\sin\phi & cb\cos\phi + cL\sin\phi \\ 0 & 1 & cL\cos\phi & -cL\cos\phi & 0 & 0 \\ 0 & 0 & * & * & cb\sin\phi + cL\cos\phi & cb\sin\phi - cL\cos\phi \\ 0 & 0 & 1 & 0 & 0 & 0 \\ 0 & 0 & 0 & 1 & 0 & 0 \end{bmatrix}$$

It is easy to check that $\frac{\partial T}{\partial x}$ has full rank[1]. Thus $T(x)$ is a valid state space transformation. The inverse transformation $x = T^{-1}(z)$ is given by

$$\begin{aligned} x_1 &= z_1 - L\cos(cz_5 - cz_6) \\ x_2 &= z_3 - L\sin(cz_5 - cz_0) \\ \theta_1 &= z_5 \\ \theta_2 &= z_6 \\ \begin{bmatrix} \eta_1 \\ \eta_2 \end{bmatrix} &= \Phi^{-1}\begin{bmatrix} z_2 \\ z_4 \end{bmatrix} \end{aligned}$$

We partition the state variable z into two blocks

$$\begin{aligned} z^1 &= [\, z_1 \;\; z_2 \;\; z_3 \;\; z_4 \,]^T \\ z^2 &= [\, z_5 \;\; z_6 \,]^T \end{aligned}$$

After applying the feedback (28), the system of the mobile robot is represented in the following normal form.

$$\dot{z}^1 = Az^1 + Bu \tag{32}$$

$$\dot{z}^2 = w(z^1,\ z^2) \tag{33}$$

$$y = Cz^1 \tag{34}$$

where

$$A = \begin{bmatrix} 0 & 1 & 0 & 0 \\ 0 & 0 & 0 & 0 \\ 0 & 0 & 0 & 1 \\ 0 & 0 & 0 & 0 \end{bmatrix}, \quad B = \begin{bmatrix} 0 & 0 \\ 1 & 0 \\ 0 & 0 \\ 0 & 1 \end{bmatrix}, \quad C = \begin{bmatrix} 1 & 0 & 0 & 0 \\ 0 & 0 & 1 & 0 \end{bmatrix}$$

[1]The terms denoted by $*$ do not affect the computation of the rank.

$$w(z^1,\ z^2) = \Phi^{-1}(z)\begin{bmatrix} z_2 \\ z_4 \end{bmatrix} =$$
$$-\frac{1}{2c^2bL}\begin{bmatrix} cb\sin\phi - cL\cos\phi & -cb\cos\phi - cL\sin\phi \\ -cb\sin\phi - cL\cos\phi & cb\cos\phi - cL\sin\phi \end{bmatrix}\begin{bmatrix} z_2 \\ z_4 \end{bmatrix}$$

It is understood that ϕ in the expression of $w(z^1,\ z^2)$ is a shorthand notation for $c(z_5 - z_6)$. Together, the linear state equation (32) and the linear output equation (34) are an equivalent representation of the input-output map (equations (29) and (30)). Equation (33) represents the unobservable internal dynamics of the mobile robot under the look-ahead control.

The zero dynamics of a control system is defined as the dynamics of the system when the outputs are identically zero (*i.e.*, $y = 0,\ \dot{y} = 0,\ \ddot{y} = 0, \ldots$). If the outputs are identically zero, it implies that $z^1 = 0$, and the zero dynamics is

$$\dot{z}^2 = w(0,\ z^2) = 0 \tag{35}$$

Thus, z^2 remains constant while the outputs are identically zero. The zero dynamics is stable but not asymptotically stable. In other words, if the reference point P_r remains still, so does the mobile robot (or more specifically, the wheels do not move).

We now look at the internal dynamics while the reference point is in motion. More specifically, we are interested in the internal motion of the mobile robot when it moves straight forward or backward. Let the mobile robot be initially headed in the positive **X** direction. We assume that the reference point is controlled to move in the negative **X** direction. The velocity of the reference point is then

$$\begin{bmatrix} \dot{y}_1 \\ \dot{y}_2 \end{bmatrix} = \begin{bmatrix} z_2 \\ z_4 \end{bmatrix} = \begin{bmatrix} -\epsilon(t) \\ 0 \end{bmatrix}$$

where $\epsilon(t) > 0$. Substituting this into the internal dynamics (33), we obtain

$$\begin{bmatrix} \dot{z}_5 \\ \dot{z}_6 \end{bmatrix} = \frac{\epsilon(t)}{2c^2bL}\begin{bmatrix} cb\sin\phi - cL\cos\phi \\ -cb\sin\phi - cL\cos\phi \end{bmatrix}$$

A solution of this internal dynamics is

$$z_5^* = -\frac{1}{r}t + c_1 \tag{36}$$

$$z_6^* = -\frac{1}{r}t + c_1 \tag{37}$$

where c_1 is a constant. That is, the two wheels rotate at exactly the same angular velocity and the mobile platform moves straight in the negative **X** direction.

We now study the stability of the internal motion described by equations (36) and (37). We first change the state variable so that the stability of the internal motion in z^2 can be formulated as the stability of equilibrium points in ζ.

$$\zeta_1 = z_5 - z_5^*$$

$$\zeta_2 = z_6 - z_6^*$$

We may express the internal dynamics in terms of $\zeta = [\ \zeta_1 \quad \zeta_2\ ]^T$.

$$\dot{\zeta} = \begin{bmatrix} \dot{\zeta}_1 \\ \dot{\zeta}_2 \end{bmatrix} = \frac{\epsilon(t)}{2c^2bL}\begin{bmatrix} cb\sin(c\zeta_1 - c\zeta_2) - cL\cos(c\zeta_1 - c\zeta_2) \\ -cb\sin(c\zeta_1 - c\zeta_2) - cL\cos(c\zeta_1 - c\zeta_2) \end{bmatrix} + \begin{bmatrix} \frac{1}{r} \\ \frac{1}{r} \end{bmatrix}$$

This system has an equilibrium subspace characterized by

$$E_\zeta = \{\zeta \mid \zeta_1 = \zeta_2\}$$

We may not draw any conclusion based on the linear approximation of the internal dynamics which has an eigenvalue at the origin. We will utilize the Liapunov method to establish the stability condition. Consider the following candidate for a Liapunov function

$$V(\zeta) = 1 - \cos(c\zeta_1 - c\zeta_2)$$

In a neighborhood of E_ζ, $V(\zeta) = 0$ if $\zeta \in E_\zeta$, and $V(\zeta) > 0$ if $\zeta \notin E_\zeta$. Thus $V(\zeta)$ is positive definite with respect to E_ζ, and may serve as a Liapunov function for testing the stability of E_ζ. We compute the derivative of $V(\zeta)$ with respect to the time

$$\dot{V}(\zeta) = \frac{\partial V}{\partial \zeta}\dot{\zeta} = \frac{\epsilon(t)}{L}\sin^2(c\zeta_1 - c\zeta_2)$$

Since $\epsilon(t) > 0$, $\dot{V}(\zeta)$ is also positive definite with respect to E_ζ. Therefore the equilibrium subspace E_ζ is not stable.

On the other hand, if the reference point is controlled to move in the positive **X** direction, the velocity of the reference point is

$$\begin{bmatrix} \dot{y}_1 \\ \dot{y}_2 \end{bmatrix} = \begin{bmatrix} \dot{z}_2 \\ \dot{z}_4 \end{bmatrix} = \begin{bmatrix} \epsilon(t) \\ 0 \end{bmatrix}$$

where $\epsilon(t) > 0$. Using the same Liapunov function, we can similarly show that

$$\dot{V}(\zeta) = -\frac{\epsilon(t)}{L}\sin^2(c\zeta_1 - c\zeta_2)$$

along the forward internal motion. Therefore, the forward internal motion is stable. Intuitively, if the mobile platform is "pushed" at the reference point, the internal motion is not stable. If it is "pulled" or "dragged" at the reference point, the internal motion is stable.

5 Simulation and Experimental Results

Simulations and experiments have been conducted to verify the theoretical analysis presented in the preceding section. In particular, simulations and experiments are focused on the verification of unstable behaviors when the mobile robot is commanded to move backward. The desired trajectory for the reference point is chosen to be

$$y_1^d(t) = -V_x t \tag{38}$$
$$y_2^d(t) = 0 \tag{39}$$

where $V_x > 0$ is the desired velocity. The following parameters are used in both simulations and experiments: $L = 0.487$ m, $b = 0.171$ m, $r = 0.0228$ m, $d = 0$ m, and $c = 0.0667$.

Depending on the initial conditions of the state variable x, the following three cases are examined in simulations and experiments:

1. The initial value of x_1 and x_2 are chosen such that the actual reference point coincides with the desired trajectory at $t = 0$, i.e.,

$$y_1(0) = y_1^d(0) = 0$$
$$y_2(0) = y_2^d(0) = 0$$

The initial values of θ_1, θ_2, η_1, and η_2 are all set to zero. Consequently, the initial heading angle is zero.

2. The initial values of θ_1 and θ_2 are chosen such that the initial heading angle $\phi(t = 0) = c(\theta_1(0) - \theta_2(0)) = 0.1$ degrees. All other initial conditions are the same as in case 1.

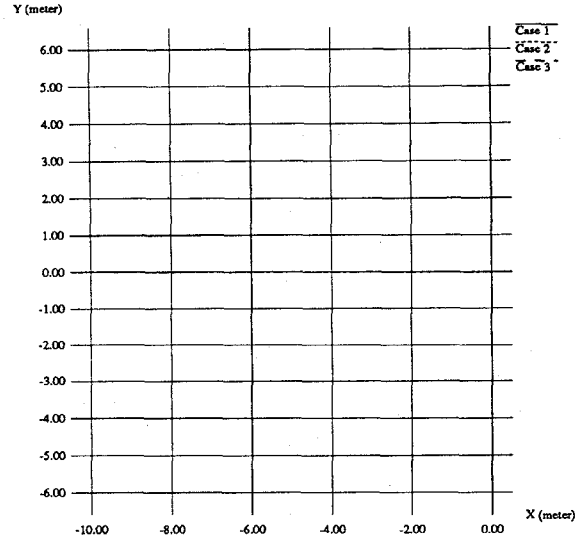

Figure 2: The actual trajectories of the reference point (simulation).

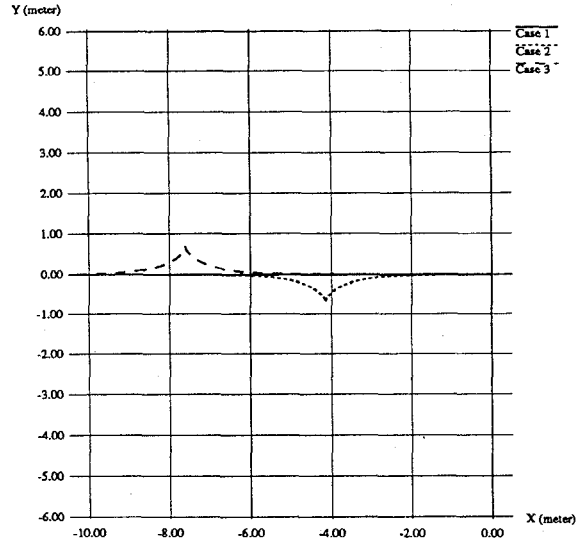

Figure 3: The trajectories of the point P_0 on the wheel axis (simulation).

3. The initial conditions are the same as in case 1. However, a disturbance in the heading angle is introduced in the middle of the trajectory. In simulations, the disturbance is introduced by adding $\Delta\phi = 0.1$ degrees to the actual heading angle for two sampling intervals 3.0 seconds later. In experiments, the disturbance is introduced by placing a copy of magazine on the floor. When one of the driving wheels runs over the magazine, the heading angle is altered slightly due to different floor conditions at the two wheels.

5.1 Simulations

Simulations are conducted with the sampling rate of 100 Hz. Figure 2 shows the actual trajectory of the reference point, and Figure 3 shows that of the point P_0 for the three cases. Figure 4 depicts the trajectory of the heading angle. In all three cases, the reference point follows the desired trajectory very closely. Nevertheless, the internal motions of the mobile platform corresponding to the three cases are distinctively different. In the first case, the mobile platform moves backward without changing the heading angle. In the second and third cases, while the reference point tracks the desired trajectory, the mobile platform itself exibits a swiveling motion and changes the heading angle by 180 degrees. To clearly see the swiveling motion, the trajectory for the third case is repeated in Figure 5 in which a box and the tip of the line extended from a corner of the box represent the platform and the reference point, respectively. Therefore, these simulation results support that the internal motion of the mobile platform when the reference point is commanded to move backward is unstable.

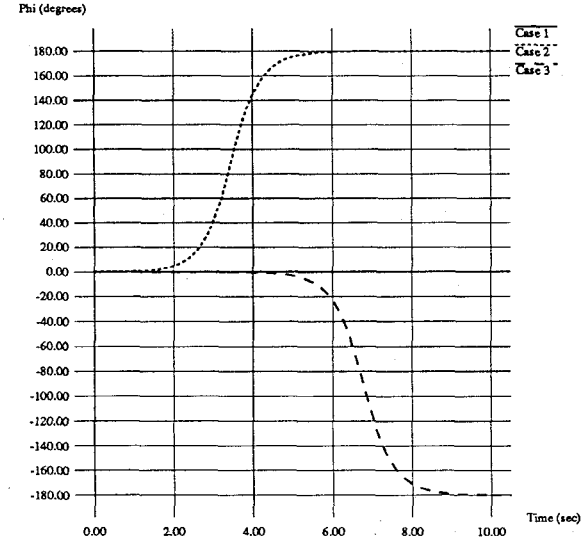

Figure 4: The heading angle of the platform (simulation).

5.2 Experiments

Experiments are conducted using a Labmate[2] mobile platform which is controlled with the sampling rate of 9 Hz. The trajectories of the reference point and the point P_0 for the three cases are shown in Figure 6 and 7, respectively. Also the trajectory of the heading angle is shown in Figure 8. The experimental results are consistent with the simulation results. While the mobile platform moves straight backward without changing the heading angle in the first case, the swiveling motions are observed in the latter two cases.

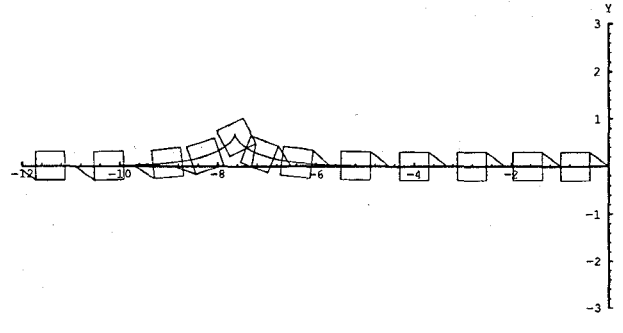

Figure 5: The trajectory of the mobile platform in Case 3 (simulation).

[2]LABMATE is a trademark of Transitions Research Corporation.

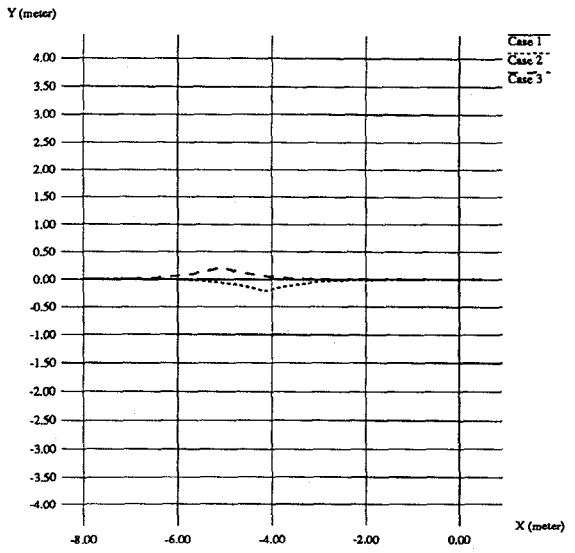

Figure 6: The actual trajectories of the reference point (experiment).

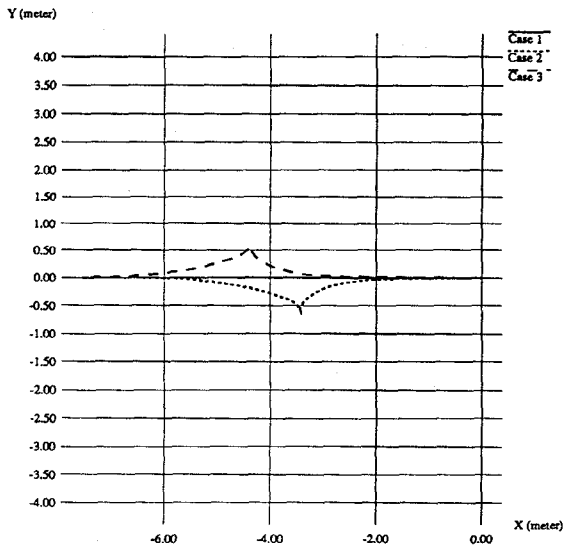

Figure 7: The trajectories of P_0 on the wheel axis (experiment).

To further demonstrate the unstable behavior of mobile platform internal motions, Figure 9 shows the experimental trajectory of the mobile platform with an initial position error in the Y-direction. In the figure, the desired trajectory (dashed line) has a small offset in the Y-direction ($\Delta Y = 7mm$) from the initial position of the Labmate. The figure shows that the platform converges on the desired trajectory while it turns around on the way.

6 Conclusion

We investigated the behavior of the internal dynamics of a wheeled mobile robot system. We showed that the internal motion of the system is asymptotically stable when the reference point is controlled to move forward, but is unstable when it is controlled to move backward. This result was confirmed by the simulation and experimental results.

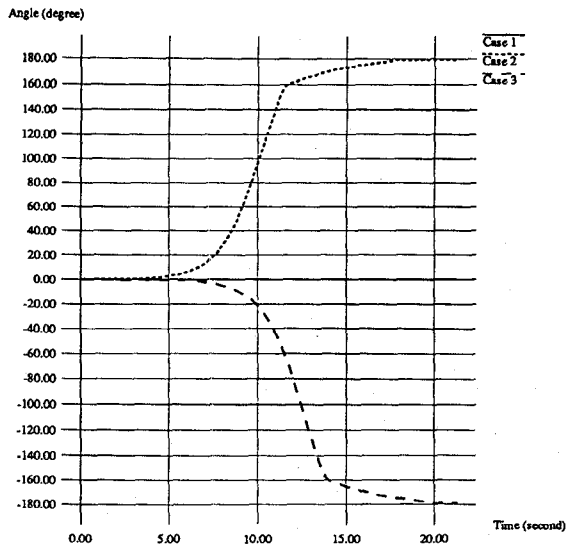

Figure 8: The heading angles of the Labmate (experiment).

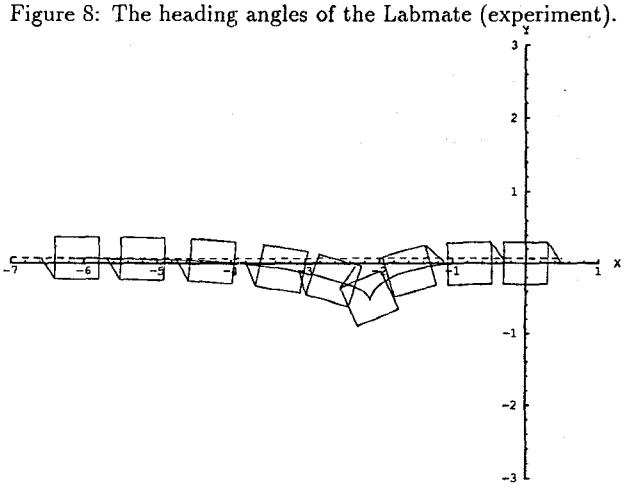

Figure 9: The trajectory of the mobile platform with an offset (experiment).

Acknowledgment

This work is in part supported by NSF grants BCS-92-16691, CDA-92-22732, CISE/CDA-90-2253, CISE/CDA 88-22719, and IRI-92-09880, ONR/DARPA grants N0014-92-J-1647 and N0014-88-K-0630, Army/DAAL grant 03-89-C-0031PRI, the Whitaker Foundation, and the University of Pennsylvania Research Foundation.

References

[1] B. d'Andrea-Novel, G. Bastin, and G. Campion. Modelling and control of non holonomic wheeled mobile robots. In *Proceedings of 1991 International Conference on Robotics and Automation*, pages 1130–1135, Sacramento, CA, April 1991.

[2] C. Samson and K. Ait-Abderrahim. Feedback control of a nonholonomic wheeled cart in cartesian space. In *Proceedings of 1991 International Conference on Robotics and Automation*, pages 1136–1141, Sacramento, CA, April 1991.

[3] C. Canudas de Wit and R. Roskam. Path following of a 2-DOF wheeled mobile robot under path and input torque constraints. In *Proceedings of 1991 International Conference on Robotics and Automation*, pages 1142–1147, Sacramento, CA, April 1991.

[4] B. d'Andrea-Novel, B. Bastin, and G. Campion. Dynamic feedback linearization of nonholonomic wheeled mobile robots. In *Proceedings of 1992 International Conference on Robotics and Automation*, pages 2527–2532, Nice, France, May 1992.

[5] A. M. Bloch and N. H. McClamroch. Control of mechanical systems with classical nonholonomic constraints. In *Proceedings of 28th IEEE Conference on Decision and Control*, pages 201–205, Tampa, FL, December 1989.

[6] A. M. Bloch, N. H. McClamroch, and M. Reyhanoglu. Controllability and stabilizability properties of a nonholonomic control system. In *Proceedings of 29th IEEE Conference on Decision and Control*, pages 1312–1314, Honolulu, HW, December 1990.

[7] A. M. Bloch, M. Reyhanoglu, and N. H. McClamroch. Control and stabilization of nonholonomic dynamic systems. *IEEE Transactions on Automatic Control*, 37(11):1746–1757, November 1992.

[8] R. W. Brockett. Asymptotic stability and feedback stabilization. In R. W. Brockett, R. S. Millman, and H. J. Sussmann, editors, *Differential Geometric Control Theory*, pages 181–191, Birkhauser, Boston, MA, 1983.

[9] Y. Yamamoto and X. Yun. Coordinating locomotion and manipulation of a mobile manipulator. In *Proceedings of 31st IEEE Conference on Decision and Control*, pages 2643–2648, Tucson, AZ, December 1992.

[10] C. Samson and K. Ait-Abderrahim. *Mobile robot control Part 1: Feedback control of non holonomic wheeled cart in Cartesian space.* Technical Report No. 1288, INRIA, Sophia-Antipolis, France, 1990.

[11] Reinhardt M. Rosenberg. *Analytical Dynamics of Discrete Systems.* Plenum Press, New York, 1977.

[12] A. Isidori. *Nonlinear Control Systems: An Introduction.* Springer-Verlag, Berlin, New York, 1985.

[13] Jean-Jacques E. Slotine and Weiping Li. *Applied Nonlinear Control.* Prentice Hall, Inc., Englewood Cliffs, New Jewsey, 1991.

[14] A. De Luca. Zero dynamics in robotic systems. In C. I. Byrnes and A. Kurzhansky, editors, *Nonlinear Systhesis*, pages 68–87, Birkhauser, Boston, MA, 1991.